

## MICROSTRUCTURAL STUDY OF AL-20SI-5FE ALLOYS PRODUCED BY MELT-SPINNING PROCESS

Aliyeh Rafiei\*, Nasser Varahram, Parviz Davami

*Department of Materials Science and Engineering, Sharif University of Technology, P.O. Box 11365-9466, Azadi Avenue, 14588 Tehran, Iran*

*Received 23.08.2012*

*Accepted 25.10.2012*

### Abstract

Al-20Si-5Fe ribbons were produced by melt spinning at the rotating speed of 20 and 40m/s. The microstructure of ribbons and conventionally cast alloys were characterized using scanning electron microscopy (SEM) together with the energy dispersive spectroscopy (EDS), X-ray diffractometry (XRD) method. The microhardness of the ribbons and as cast ingots was also measured. SEM observations showed that the wheel side of the ribbons exhibited a finer microstructure than those on the air side which exposed to the atmosphere. The phase constitution of the hypereutectic Al-20Si-5Fe alloy was considerably affected by rapid solidification. XRD results showed that the phases present in the as cast hypereutectic Al-20Si-5Fe alloy were identified to be  $\alpha$ -Al, Si and intermetallic  $\beta$ -Al<sub>5</sub>FeSi phases while only  $\alpha$ -Al and Si were identified in the melt spun ribbons. Moreover, the values of Vickers microhardness of melt spun ribbons were three times as high as those of conventionally cast ingots of the same alloy.

*Keywords: Melt-Spinning, Al-20Si-5Fe alloy, Microstructure, Rapid Solidification, Microhardness*

### Introduction

Al-Si alloys have extensive applications in automotive, electrical and aerospace industries due to their unique properties such as excellent castability, wear resistance, light weight and low coefficient of thermal expansion [1-5]. There is an increasing demand for hypereutectic Al-Si alloys as a substitute for hypoeutectic Al-Si alloys because a higher volume fraction of silicon leads to excellent mechanical properties [6, 7]. Besides, third element addition to Al-Si alloys such as iron and other transition elements [8-12] improves strength, wear resistance and thermal stability. That is due to the formation of hard iron-containing intermetallic compounds [13-16]. Nevertheless,

---

\* Corresponding author: Aliyeh Rafiei, aliyeh.rafiei@gmail.com

increasing the silicon content and addition of iron bring about some problems. Increasing silicon content above the eutectic composition, because of the formation of coarse primary silicon particles lead to poor mechanical properties of the Al-Si alloys. In the case of iron addition, formation of intermetallic compounds with acicular morphology can considerably deteriorate fracture toughness and ductility [17-21]. For these reasons, size, shape and distribution of primary silicon particles and intermetallics determine the mechanical properties of these alloys [22].

Over the past few decades, a significant quantity of research has been done to investigate the influence of rapid solidification on the microstructure and properties of hypereutectic Al-Si alloys. Among various rapid solidification techniques, gas atomization [23], spray deposition [4, 24] and melt spinning [25] have been studied extensively. It is well demonstrated that rapid solidification of hypereutectic Al-Si alloys through high cooling rates permits the enhancement of alloy properties by refinement of microstructure, extension of solid solubility, uniform distribution of the second phases, formation of metastable crystalline alloys and supersaturated solid solutions [26-29].

In the present study, the microstructural characteristics of melt-spun Al-20wt.%Si-5wt.%Fe alloy were characterized by examining the solidification morphology of the ribbons and compared with those produced under conventional conditions (as cast). For this purpose, scanning electron microscopy (SEM) and X-ray diffraction techniques were carried out on the alloy. The microhardness values of the ribbons and as-cast specimens were also measured.

### **Materials and methods**

Al-20Si-5Fe alloy (nominal composition in wt%) was prepared by induction melting of commercially pure metals in a graphite crucible in air atmosphere. Molten alloy poured in cylindrical moulds having the diameter of 45 mm and height of 350 to produce conventionally cast samples. After remelting alloy in a quartz tube for an hour, the melt spun ribbons were produced by using a single roller type melt spinning device. Rapidly solidified ribbons were produced by free jet melt spinning in Argon protective gas by means of impinging a jet of molten metal from a nozzle having the diameter of 700 $\mu$ m onto the cylindrical surface of a copper wheel (24 cm in diameter) at rotating speed of 20 and 40 m/s. The distance between nozzle and wheel was fixed on 2.5mm. The temperature before ejection was 820°C, which is approximately 100°C above the liquidus temperature of the materials. The thickness of ribbons was 30 $\mu$ m, on average. The microstructural examinations were performed by scanning electron microscopy (Tescan VEGAII XMU, Czech Republic) operated at 15 kV and linked with an Energy Dispersive Spectrometry (EDS) attachment. The XRD measurements were conducted in X-ray diffraction (XRD, Philips Xpert) using Cu K $\alpha$  radiation ( $\lambda=1.5406$  Å) at 2 $\theta$  step of 0.02° and scanning duration of 1 s from 10° to 80°. Using standard metallographic techniques followed by chemical etching in a 0.5% HF solution for about 5s, mounted specimens were prepared for SEM investigations. The hardness of the ribbons and as cast ingots measured with a Vickers diamond indenter in a microhardness tester (Micromet 2100, Buehler, USA) at applied load of 10 g.

## Results

### XRD Studies

Figure 1 illustrates the X-Ray diffraction (XRD) pattern taken from ingot Al-20Si-5Fe alloy. The XRD pattern indicates that conventionally cast alloy is composed of  $\alpha$ -Al, Si and intermetallic phase ( $\beta$ -Al<sub>5</sub>FeSi). This result is consistent with electron microscopy observations. The peaks related to intermetallic phase ( $\beta$ -Al<sub>5</sub>FeSi) between Al and Si is disappeared in Figs. 2 a, b, for the melt-spun ribbons. The absence of the intermetallic phase in X-ray diffraction pattern also reveals the extended solid solubility of the matrix. The presence of low intensity Si peaks indicates that there is still some undissolved Si in the aluminum matrix. However, the absence of peaks related to other elements may not point out to complete solution of other elements, e.g. Fe. It should be also considered that the detection limit by X-ray diffraction technique (XRD) is typically about 5 vol.%.

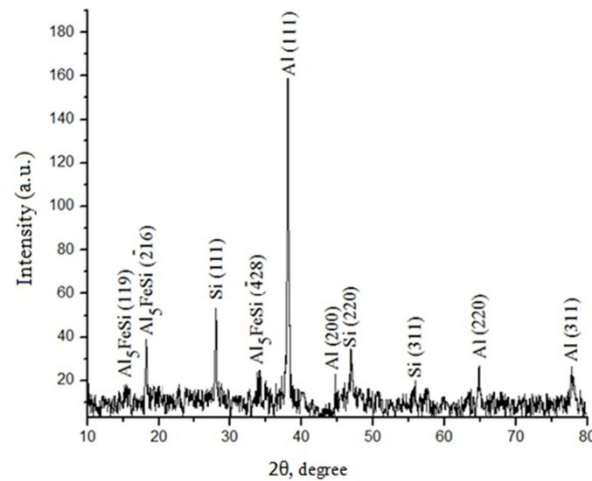


Fig. 1. XRD pattern taken from the ingot Al-20Si-5Fe alloy.

According to the X-ray diffraction patterns, it was resulted that at the high cooling rates, the aluminum matrix undergoes a supersaturation. Solid solubility extension of Si in the aluminum matrix and absence of intermetallic phases as a consequence of rapid solidification have been reported previously [8, 25, 30, 31, 32]. The shift in the (111) and (200) diffraction lines of Al indicated lattice parameter of 0.40371nm and 0.40393nm for the wheel and free-side of the ribbon. By using the intercept method [33] a solid solubility extension of 7.3 at.% and 5.2 at.% for silicon was estimated. These values are close to those reported by Birol [34] but higher than those stated by Öveçoğlu et al. [35] which is attributed to different chemical compositions and cooling rates (melt-spinning conditions) used in the present work.

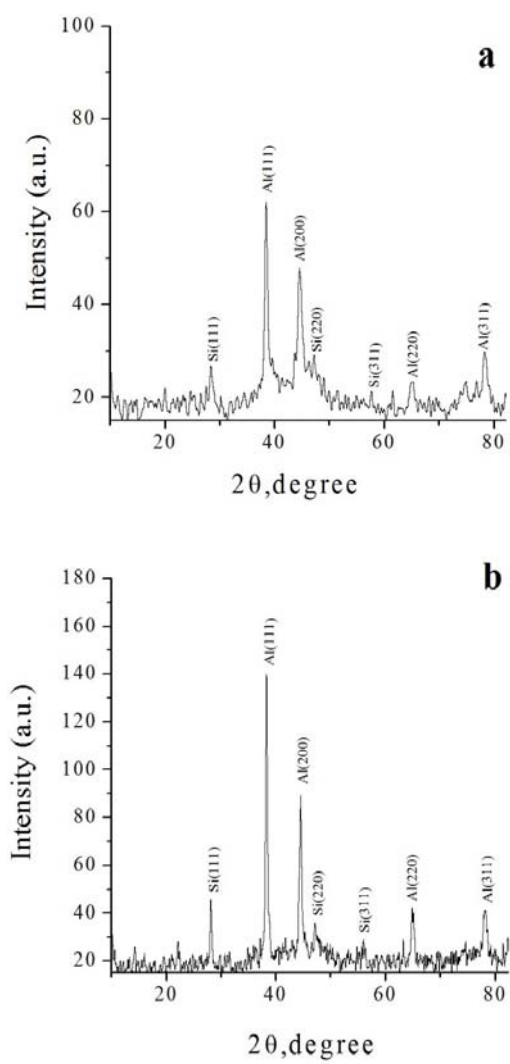
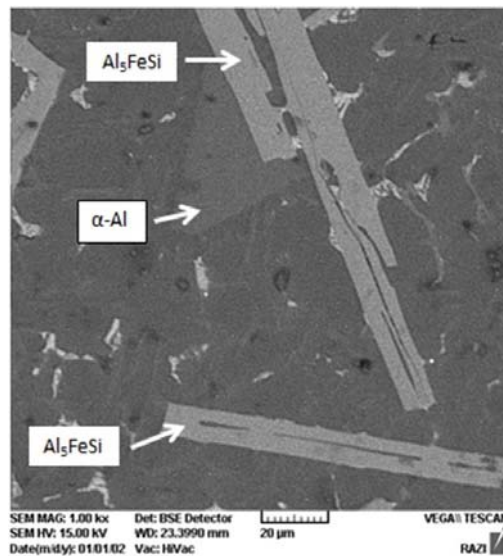


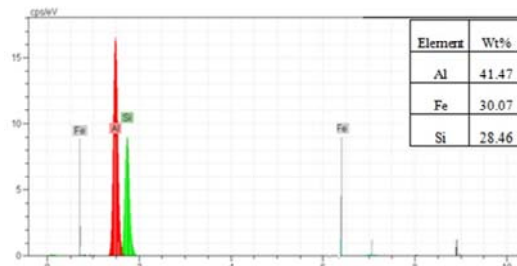
Fig.2. XRD pattern taken from melt-spun ribbons produced at a) 20m/s, b) 40m/s.

*Microstructural investigations*

Microstructural investigations showed that the structure of melt spun ribbons was completely different from their conventionally cast counterparts. The microstructure of as cast Al-20Si-5Fe alloy is shown in Fig.3. It is obviously seen that the microstructure consists of coarse  $\alpha$ -Al dendrites together with coarse blocky region of primary Si. Furthermore, coarse disordered intermetallic phase ( $\beta$ -Al<sub>5</sub>FeSi) was distinguished in the  $\alpha$ -Al matrix.



(3.a)



(3.b)

Fig.3. a) SEM micrograph of as-cast Al-20Si-5Fe alloy; needle like Al<sub>5</sub>FeSi phase and  $\alpha$ -Al are shown by arrows. b) EDS analysis of needle like intermetallics shown in micrograph (a).

The microstructure of the cross section of the melt spun ribbons is shown in Fig. 4. The wheel side of ribbons exhibits a featureless region (A in Fig. 4). with an average thickness of 10 $\mu$ m. The solidification of this zone is diffusionless due to the highest cooling rate at chilling surface hence this region appears featureless after etching [36]. The formation of this zone is consistent with the result of Delhez et al. work [37]. As

the distance from wheel side increases, the cooling rate decreases and microstructure becomes coarser. Immediately after featureless zone, there is a transition region (B in Fig. 4) with a columnar structure including the columnar grains perpendicular to the wheel surface. This region is a transition between featureless and free (air) side. In general, the thickness of the columnar region decreases with increasing alloying element levels. Thus, in the present work, the small thickness of transition region could be attributed to the high level of alloying elements. Van Rooyen et al. had reported that the presence of second phases at grain boundaries reduces the thickness of columnar region [38]. Finally, at the free surface, which is in contact with atmosphere, there is a dendritic region (C in Fig. 4) which consists of Al-rich dendrites. Solidification rate at this region is slower than the second one, so the columnar grains disappear and dendritic structure appears as the main structure [32].

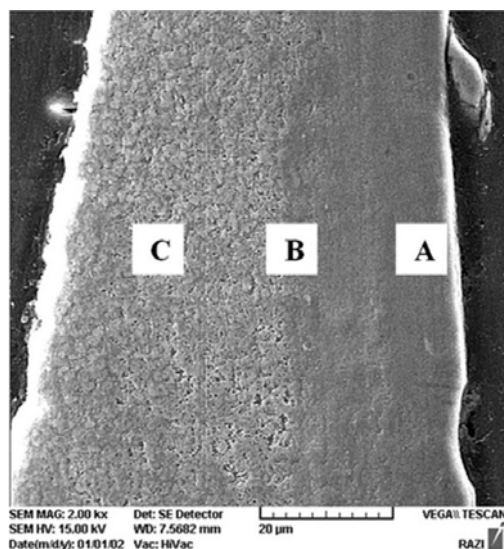
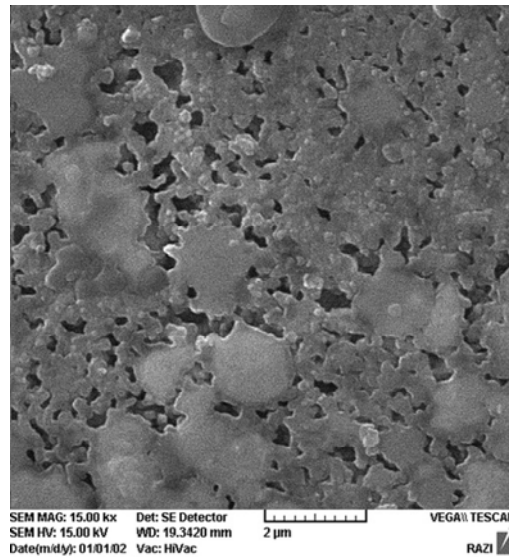


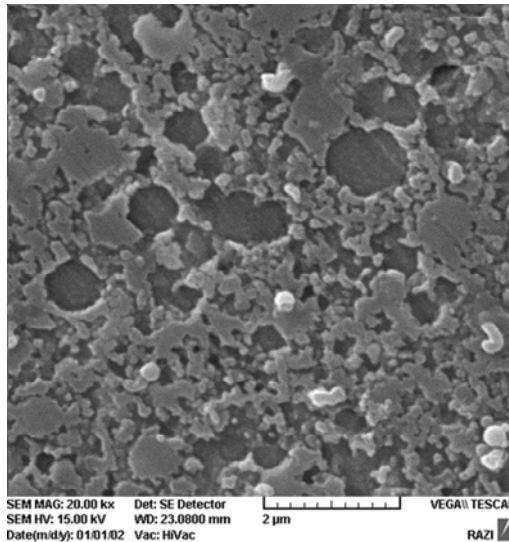
Fig.4. Cross sectional micrograph of the melt-spun Al-20Si-5Fe ribbon. A) Featureless Region, B) Transition Region, C) Dendritic Region.

Rapid solidification process changes the phase constitution and also has a striking effect on the microstructure of the Al-20Si-5Fe alloy. Figs. 5 a, b represent the SEM micrographs of the melt-spun Al-20Si-5Fe ribbons rapidly solidified at rotating speed of 20 and 40m/s. The Si particle size is reduced and their numbers increase with increasing solidification rate. As seen in Fig. 5a, a relative large amount of the dendrite Si phase and  $\alpha$ -Al phase exists in the sample at lower rotating speed (20m/s). Moreover, Fig. 5a also shows some morphological details of these dendrites with the size approximately above the range of 3 $\mu$ m size. The results show that the microstructures of all melt-spun ribbon is completely composed of finely dispersed  $\alpha$ -Al and dendrite Si phase. While in the specimen solidified at high rotating speed of 40 m/s, dendrites disappear and very fine homogeneous structure is revealed, as seen in Fig. 5b. Obviously, a higher solidification rate leads to smaller grain size and increase in particles number. It indicates that the high solidification rate of melt spinning process effectively improves the composition homogeneity of the alloy. Furthermore, SEM

results indicated that the microstructure of melt spun alloy formed at the relative lower rotating speed (20m/s) was of dendrite structure and for the alloy formed at a relative higher rotating speed (40m/s) was of very homogeneous structure, and both had a more uniform composition than their conventionally cast counterparts.



a)



b)

*Fig.5. SEM micrograph of melt-spun Al-20Si-5Fe ribbons produced at a) 20m/s and b) 40m/s.*

### Effect of cooling rate on the thickness of ribbons

The thickness of achieved ribbons was 40 to 80  $\mu\text{m}$  and 15 to 35  $\mu\text{m}$ , for the rotating speeds of 20 and 40 m/s, respectively. It can be presumed that in the melt spinning process, the thickness of the obtained ribbons is indicative of the average cooling rate, provided that the experimental conditions are reasonably constant. The thickness of ribbons is directly proportional to the rate at which the ribbon cooled. A fast cooling rate (i.e. a higher disk rotation) will result in a thinner ribbon formation [39].

### Microhardness

The microhardness ( $H_v$ ) of the directionally solidified materials also depends on the solidification parameters, such as cooling rate. In the present work, the microhardness of conventionally cast ingot and rapidly solidified ribbons were calculated by Vickers microhardness measurements. The applied load to determine the hardness was 10 g, as performed on previous works [9, 39, 40]. On the longitudinal section of each ribbon, 7 measurements were performed. The comparison of Vickers microhardness values of ribbons and ingot is shown in Fig.6. It indicates that the hardness of the melt-spun ribbons produced at the rotating speeds of 20 and 40 m/s is approximately 3 and 4 times higher than those of original ingot alloy, respectively. The particle size of rapidly solidified ribbons is much smaller compared with the particle size of those cast under conventional condition as mentioned before. Hence, increase in hardness values for melt spun alloys compared with their as cast counterparts can be attributed to supersaturated solid solution of  $\alpha\text{-Al}$ , grain refinement and changes in microstructure occurred during the melt spinning process. The atomic radius difference between five elements in solid solution creates a strain field, which interacts with dislocations. The solid solution strengthening mechanism is also supported by the XRD analyses and SEM observations.

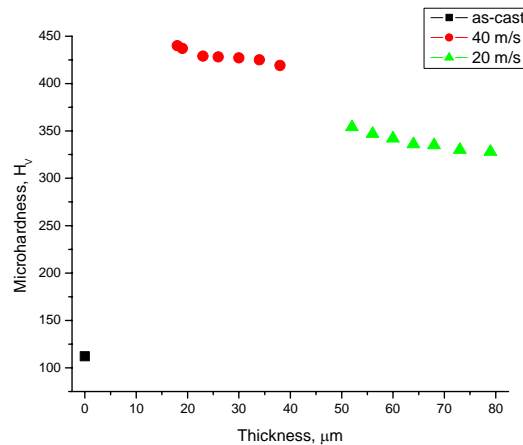


Fig.6. Microhardness as a function of thickness of ribbons.

## Conclusions

According to the present work, the results can be summarized as follow:

The microstructure of as melt spun state exhibited enhanced properties compared to the as-cast structure of this alloy, including homogeneity and grain refinement.

Extension of solid solubility of Si in the Al matrix was observed.

SEM images showed that the microstructure of rapidly solidified ribbons only consisted of  $\alpha$ -Al and Si phases and no intermetallic phases was revealed due to extension of solid solubility and high cooling rates.

The microstructure of the melt-spun ribbons exhibited a featureless zone caused by high cooling rate and a dendritic zone in the air-side due to the lower cooling rates.

The increase in cooling rate led to the increase in microhardness, so that it was 3 to 4 times higher than those conventionally cast ingots.

## Acknowledgement

The authors are grateful to thank supports of Razi Metallurgical Research Center (RMRC) and Materials Science and Engineering department of Sharif University of Technology.

## References

- [1] Y. Wang, Z. Zhang, H. Geng, W. Wang, X. Bian, Mater. Sci. Eng. A 427 (2006) 203–209.
- [2] J. Shen, Z. Xie, Y. Gao, B. Zhou, Q. Li, J. Mater. Sci. Lett. 20 (2001) 1513–1550.
- [3] F. Wang, B. Yang, X.J. Duan, B.Q. Xiong, J.S. Zhang, J. Mater. Process. Technol. 137(2003) 191–194.
- [4] F. Wang, Z. Zhang, Y. Ma, Y. Jin, Mater. Lett. 58 (2004) 2442–2446.
- [5] V.C. Srivastava, P. Ghosal, S.N. Ojha, Mater. Lett. 56 (2002) 797–801.
- [6] N. Kuroishi, J. Mater. Process. Technol. 42 (2001) 397–401.
- [7] H. Yamagata, Mater. Sci. Forum 797 (1999) 304–306.
- [8] N. Unlu, A. Genc, M.L. Ovecoglu, N. Eruslu, F.H. Froes, J. Alloys Compd. 322 (2001) 249–256.
- [9] N. Unlu, A. Genc, M.L. Ovecoglu, E.J. Lavernia, F.H. Froes, J. Alloys Compd. 343 (2002) 223–233.
- [10] J. Zhou, J. Duszczek, B.M. Korevaar, J. Mater. Sci. 26 (1991) 824–834.
- [11] T. Hirano, In: Proceedings of 1993 Powder Metallurgy World Congress. Eds.: Y. Bando, K. Kosuge, Japanese Society of Powder and Powder Metallurgy, 1993, pp. 563–566.
- [12] T. Hirano, F. Ohmi, S. Morie, F. Kiyoto, T. Fujito, In: Proceedings of the International Conference on Rapidly Solidified Materials. Eds.: P.W. Lee, R.S. Carbonara, San Diego, California, American Society for Metals, 1985, pp. 327–339.
- [13] J.M. Sater, T.H. Sanders, R.K. Garrett, Rapidly Solidified Powder Aluminium Alloys Symp. (1984) 83–117.
- [14] T. Hayashi et al., Sumitomo Electric Tech. 34 (1992) 107.
- [15] N. Amano et al., Metal Powder Rep. 38 (1983) 186.

- [16] L. Wange, M. Makhlof, D. Apelian, Worcester Polytechnic Int. Worcester, (1993) 150–165.
- [17] S.G. Shabestari, Mater. Sci. Eng. A 383 (2004) 289–298.
- [18] T.O. Mbuya, B.O. Odera, S.P. Nganga, Int. J. Cast Met. Res. 16 (2003) 1–15.
- [19] S.G. Shabestari, J.E. Gruzleski, AFS Trans. 26 (1995) 285–293.
- [20] B. Kulunk, S.G. Shabestari, J.E. Gruzleski, D.J. Zuliani, AFS Trans. 170 (1996) 1189–1193.
- [22] M. Rajabi, A. Simchi, M. Vahidi, P. Davami, J. Alloys Compd. 343 (2008) 223–233.
- [23] P. Skjerpe, Metall. Trans. A 18A (1987) 189–200.
- [24] R. Trivedi, F. Jin, I. Anderson, Acta Mater. 51 (2003) 289–300.
- [25] A. Srivastava, V. Srivastava, A. Gloter, S. Ojha, Acta Mater. 54 (2006) 1741–1748.
- [26] M. Rajabi, M. Vhidi, A. Simchi, P. Davami, Mat. Char. 60 (2009) 1370 – 1381.
- [27] S. Hong, C. Suryanarayana, Metall. Trans. 36A (2005) 715–723.
- [28] L. A. Davis, S. K. Das, J. C. M. Li, M. S. Zedalis, Int. J. Rapid Solid. 8 (1994) 73–131.
- [29] C.J. Kong, P.D. Brown, A. Horlock, S.J. Harris, D.G. McCartney, Mater. Sci. Eng. A 375–377 (2004) 595–598.
- [30] S. S. Cho, B. S. Chun, C. W. Won, H. K. Kim, B. S. Lee, K. H. Yim, S. H. Eom, H. Back, B. J. Song, C. Suryanarayana, J. Synth. Process. 6 (1998) 123–131.
- [31] M. Salehi, K. Dehghani, J. Alloys Compd. 457 (2008) 357–361.
- [32] O. Uzun, F. Yılmaz, U. Kolemen, N. Basman, J. Alloys Compd. 509 (2011) 21–26.
- [33] M. Rajabi, A. Simchi, P. Davami, Mater. Sci. Eng. A 492 (2008) 443–449.
- [34] R. L. Snyder, J. Fiala, H. J. Bunge, Oxford University Press Inc, New York, 1999.
- [35] Y. Birol, J. Alloys Compd. 439 (2007) 81–86.
- [36] M.L. Öveçoğlu, N. Ünlü, N. Eruslu, A. Genç, Mater. Lett. 57 (2003) 3296–3301.
- [37] O. Uzun, T. Karaaslan, M. Keskin, J. Alloys Compd. 358 (2003) 104–111.
- [38] R. Delhez, Th. De Keijser, E.J. Mittemeijer, P. Van Mourik, N.M. Van Der Pers, L. Katgerman, N.E. Zalm, J. Mater. Sci. 17 (1982) 2887–2894.
- [39] M. Van Rooyen, N.M. Van Der Per, L. Katgerman, Th. De Keijser, E.J. Mittemeijer, in: S. Steeb, H. Warlimont (Eds.), Rapidly Quenched Metals, Amsterdam, The Netherlands (1985) 823–826.
- [40] A. Bendijk, R. Delhez, L. Katgerman, Th. H. De Keijser, E. J. Mittemeijer, N. M. Van Der Pers, J. Mater. Sci. 15 (1980) 2803–2810.
- [41] E. Karakose, M. Keskin, J. Alloys Compd. 479 (2009) 230–236.